LASER COMPRESSION OF MONOCRYSTALLINE TANTALUM

C. H. Lu[1], B. A. Remington[2], B. R. Maddox[2], B. Kad[1], H. S. Park[2], S. T. Prisbrey[2], R. Luo[1] and M. A. Meyers[1]

[1]*University of California, San Diego, La Jolla, CA, 92093, USA*
[2] *Lawrence Livermore National Laboratory, Livermore, CA, 94550, USA*

Abstract. Monocrystalline tantalum with orientations [100] and [111] was subjected to laser driven compression at laser energies of 350 to 685 J, generating shock amplitudes varying from 15 to 100 GPa. The laser beam, with a beam spot diameter of ~1 mm, created a crater of significant depth (~ 80 to ~ 200 μm). Twins were observed just below the crater surface (~ 42 μm) by back-scattered SEM. Transmission electron microscopy (TEM) revealed profuse mechanical twinning within a distance from the energy deposition surface of ~ 1.5 mm at 684 J compression power, corresponding to an approximate pressure of 35 GPa. The decay of the pulse through the specimens was accompanied by an attendant decrease in the density of shock-generated dislocations. Microhardness measurements were conducted on the recovered samples. The experimentally measured dislocation densities and threshold stress for twinning are compared with predictions using analyses based on the constitutive response and the similarities and differences are discussed in terms of the mechanisms of defect generation.

Keywords: Tantalum, single crystal, laser shock.
PACS: 61.50.-f, 61.72.-y, 61.72.Bb, 61.72.Qq.

INTRODUCTION

A systematic inquiry into the effects of laser pulses on FCC metals (Cu and Cu–Al) was initiated in 2001 and has yielded significant results that have been explained in terms of shock compression [1-3]. This work was extended to nickel by Jarmakani, et al. [4].

The objective of this study is to extend the methodology developed for Cu and Ni to a model BCC metal, tantalum. There are important fundamental differences between FCC and BCC metals, and the Peierls-Nabarro barrier is significantly different. In tantalum, the Peierls-Nabarro stress is ~ 2.97 GPa [5], whereas it is only ~ 120 MPa in copper [6].

EXPERIMENTAL PROCEDURE

The cylindrical tantalum monocrystals, with dimensions 3 mm diameter x 3 mm height, were placed behind a tantalum washer, inside a stainless steel recovery container. The inside of this container was filled with Aerogel, which acts as a deceleration medium for the tantalum specimens, after laser compression. The recovery container was designed to fit into the Omega chamber. Laser energy was applied by the simultaneous activation of six laser beams. A phase plate was used to smooth the laser beams. The schematic of the target holder with the tantalum specimen is shown in Fig. 1. A 180 μm BrCH (2%) reservoir covered by a 20 μm polycarbonate ablator provided the quasi-isentropic loading. The ablator, hit by six laser beams, created a quasi-isentropic loading on the first ~ 40 μm of the tantalum, after which the ramp wave steepens into a shock. The diameter of the laser beams was approximately 1 mm. The specimens were successfully recovered in this geometry. The aerogel did not introduce any

Shock Compression of Condensed Matter - 2011
AIP Conf. Proc. 1426, 1391-1394 (2012); doi: 10.1063/1.3686541

additional damage into the recovered samples and acted as a gradual decelerating medium.

RESULTS AND DISCUSSION

Five experiments on monocrystals and three complementary VISAR experiments were performed. The VISAR experiments were conducted on Al-LiF drive calibration samples and provided interface velocity data that allowed pressure versus time of the loading to be deduced, which became the input to the subsequent computer simulations. The total laser energies varied between 350 J and 680 J. The laser energy impact produced a significant cratering in the specimen surfaces. Figure 2 shows the crater, and SEM observations of the surfaces for [100] monocrystals, 661 J laser energy. The crater radius is ~ 1.2 mm in all cases, but the depth is a function of laser energy, being approximately 0.08 mm for the 350 J energy and ~ 0.18 mm for the 680 J energy level, respectively.

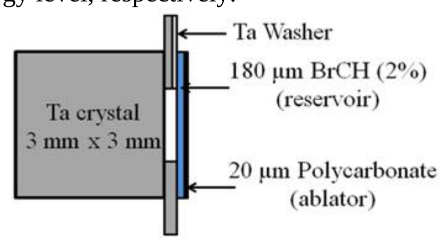

Figure 1. Monocrystalline Ta specimen and laser energy deposition assembly for quasi-isentropic compression.

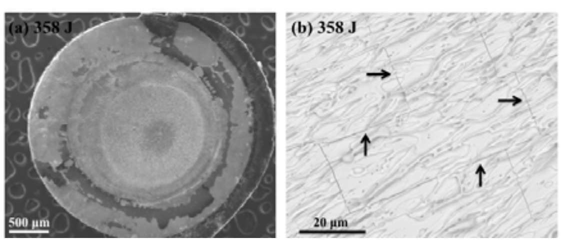

Figure 2. Surface of Ta [100] monocrystals after laser compression at 661 J; (a) optical micrographs; (b) SEM showing cracks.

The initial pressure pulse was calibrated using the VISAR traces of the Al-LiF witness plate interface velocity obtained from independent experiments under similar laser energy conditions. The initial LASNEX computed energy was corrected by a factor of 0.7 to account for 2D effects in a 1D simulation and to obtain a good fit. For distances of 5 and 10 µm from the energy deposition surface, the quasi-isentropic loading condition prevails, providing a gradual temperature rise. By the time the stress wave has penetrated 50 µm into the sample, the temperature rise is much more rapid. The steep rise in temperature at 20-30 ns for depths of 5 and 10 µm into the sample is due to the diffusive heat wave transporting into the Ta from the drive plasma stagnation at the surface. We confine our analyses to depths of 25 µm or greater into the Ta, so as to not be contaminated by this surface heat source.

Figure 3 shows the calculated pressure decay using the LASNEX hydrocode and assuming a one-dimensional propagation. The radial release is not incorporated into the calculation, which is reasonable for times under a microsecond in our experimental set-up. The pressure-time profiles at different depths are shown in Figs. 3(a) and (b) for laser energy levels of 358 J and 684 J, respectively. The pressure decays rapidly but is still significant at the back surface of the specimen (3 mm). At the same time, the pulse, that has a characteristic triangular shape, widens. For the 358 J (Fig. 3(a)) experiment, the pressure decays from ~ 50 GPa to ~ 10 GPa. For the 684 J (Fig. 3(b)) experiment, it decays from ~ 100 GPa to ~ 20 GPa.

Figure 4 shows the characteristic dislocation structure at pressures below 35 GPa for the 606 J (1.3 mm from surface). The dislocation density decreases with pressure decrease. Closer to the surface (590 µm) the SEM of Fig. 5 shows twins (same 606 J experiment).

Figure 6 shows the hardness as a function of pressure for the different experiments. There is consistency for the five experiments. The dislocation density was calculated from TEM pictures and the results are shown in Fig. 7 as a function of pressure. (Determined by VISAR measurements). The dislocation density is considerably lower than the predictions from homogeneous dislocation generation and match rather well recent predictions by Barton, et al. [7] somewhat better than the ones using Kocks'[8] equation. We conclude that Orowan dislocation multiplication, and not homogeneous dislocation generation, is the mechanism operating in Ta.

The slip-twinning transition pressure can be obtained from the analysis presented by Meyers et al. [9] for monocrystals. The slip stress is expressed by the Zerilli-Armstrong equation for BCC metals [10] and the twinning stress by the Armstrong-Worthington equation [11]. The stresses arte related to the shock pressure through the Swegle-Grady equation with coefficients from Furnish [12]. The modeling results are shown in Fig. 8 for the monocrystals. The slip-twinning transition stress is over 35-78 GPa. In the experiment at 606 J laser energy, the peak pressures in the characterized foils was ~35 GPa. This transition is manifested by an abrupt increase in hardness in Fig. 6. Thus, the model results are consistent with the experimental observations.

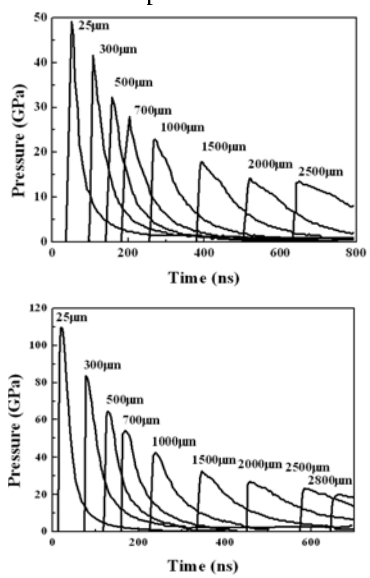

Figure 3. LASNEX simulations of the decay of the laser-generated pressure pulse as it travels through [100] tantalum specimen for (a) total laser energy of 358 J; (b) and total laser energy of 684 J.

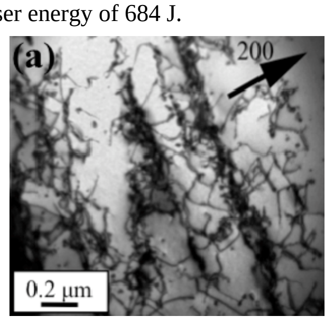

Figure 4. TEM micrograph at a distance from the laser deposition surface of 1.3 mm for [100] Ta single crystal, driven with laser energy of 606 J.

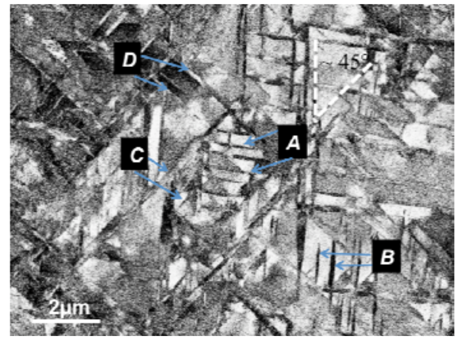

Figure 5. Twins imaged by SEM-BSE (20 kV) in [100] Ta at laser energy of 606 J; (~ 590 µm from laser shock surface).

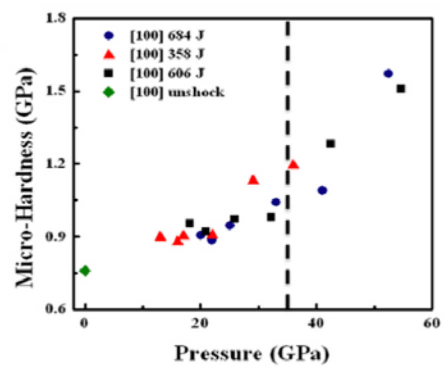

Figure 6. Hardness vs. pressure for all five experiments; notice increase beyond 35 GPa from twinning.

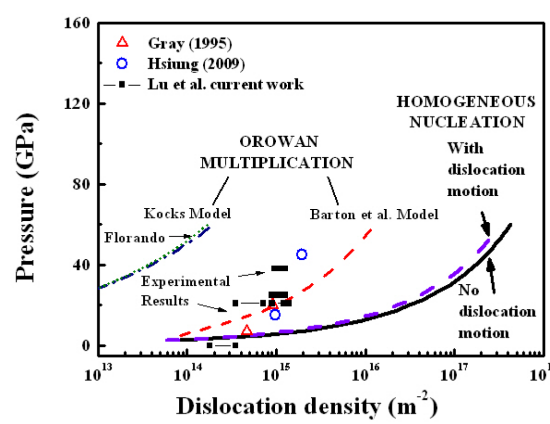

Figure 7. Dislocation density calculated from TEM images vs. Pressure and comparison with Orowan equation.

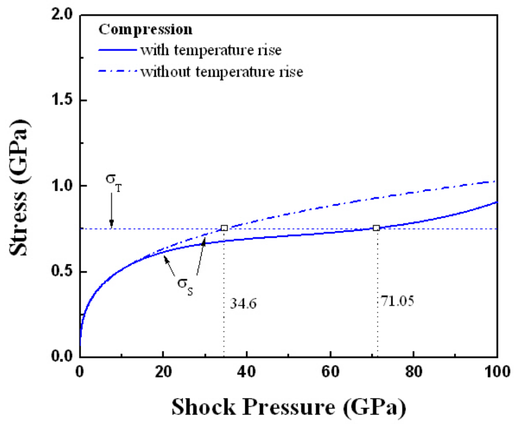

Figure 8. Slip and twinning stress is a function of shock pressure. The slip-twinning transition is in range 35-70 GPa.

CONCLUSIONS

1. [001] Ta crystals were subjected to laser compression at energies between 350 to 685 J. The dislocation density increased with the proximity to the energy deposition surface. The experimentally observed dislocation density was compared with calculations based on homogeneous dislocation generation and the results are different by orders of magnitude. These results parallel earlier investigations on copper (an FCC metal). The lower dislocation density observed experimentally might be due to two reasons: (a) dislocations are not homogeneously nucleated but rather increase their density as a result of movement, interaction, and multiplication from existing sources; (b) a significant fraction of the dislocations generated in shock compression are annihilated upon release.
2. In the proximity of the energy-deposition surface as the shock pressure raises the dislocations give way to mechanical twinning as the principal deformation mode. The experimentally obtained slip-twinning threshold stress is ~ 35 GPa. Calculations involving constitutive equations for slip and twinning and the Swegle-Grady equation predict a pressure ~ 35 GPa range, consistently with experimental results.

ACKNOWLEDGEMENTS

This work was performed under the auspices of the UC Research Laboratories (UCRL) Grant and the National Laser Users Facility (NLUF) Grant. Electron Microscopy was conducted at the SHaRE User Facility, which is sponsored at ORNL by the Division of Scientific User Facility, US Department of Energy.

REFERENCES

1. Meyers, M. A., et al., "Laser-induced shock compression of monocrystalline copper: characterization and analysis," Acta Mater **51**, 1211 (2003).
2. Meyers, M. A., et al., "Deformation substructures and their transitions in laser shock-compressed copper-aluminum alloys," Metall. Mater. Trans. A **39A**, 304 (2008).
3. Schneider, M. S., et al., "Laser shock compression of copper and copper–aluminum alloys," Int. J. Impact. Eng. **21**, 473 (2005).
4. Jarmakani, H. N., et al., "Molecular dynamics simulations of shock compression of nickel: From monocrystals to nanocrystals," Acta Mater. **56**, 5584 (2008).
5. Bechtold, J. H. "Tensile properties of annealed tantalum at low temperatures," Acta Metall. Mater. **3**, 249 (1955).
6. Cheung, K. S. and Yip, S., "A molecular-dynamics simulation of crack-tip extension: The brittle-to-ductile transition," Modell. Simul. Mater. Sci. Eng. **2**, 865 (1994).
7. Barton, N. R., et al., "A multiscale strength model for extreme loading conditions," J. Appl. Phys. **109**, 073501 (2011).
8. Kocks, U. F., "Laws for work-hardening and low-temperature creep", Trans. ASME **98**, 76, 1976.
9. Meyers, M. A., et al., "Laser compression of monocrystalline tantalum," Presented at the 2011 APS SCCM, Chicago.
10. Zerilli, F. J., et al., "Description of tantalum deformation behavior by dislocation mechanics based constitutive relations," J. Appl. Phys. **68**, 1580 (1990).
11. Armstrong, R. W. and Worthington, P. J., "Constitutive relation for deformation twinning in body centered cubic metals," Met. Eff. High Strain Rates, Proc. Tech. Conf. **401**, (1973).
12. Furnish, M. D., Chhabildas, L. C., and Steinberg, D. J., "Dynamical behavior of tantalum," AIP Conf. Proc. **309**, 1099 (1994).